Available online at www.sciencedirect.com

ScienceDirect

Journal of Magnesium and Alloys 8 (2020) 452–460

www.elsevier.com/locate/jma

Full Length Article

Mechanical and corrosion behaviour of hydroxyapatite reinforced Mg-Sn alloy composite by squeeze casting for biomedical applications

R Radha, D. Sreekanth*

School of Mechanical and Building Sciences, Vellore Institute of Technology, Chennai 600127, India

Received 25 March 2019; received in revised form 26 April 2019; accepted 21 May 2019
Available online 24 September 2019

Abstract

Magnesium alloys have gained increasing attention for biomedical applications due to their biocompatibility and the biodegradability. Hydroxyapatite (HA) is known to be a highly bioactive because of its similar chemical and crystallographic structures to bone. Therefore, HA is believed to be a potential ceramic material for the fabrication of Mg based composites, to combine the advantages of both Mg and HA. But, in general, the composites known to be more susceptible to corrosion attack than the matrix alloy. Hence, in the present work, Sn is used as an alloying element to evaluate its effect on mechanical as well as corrosion properties of Mg/HA composites. Mg with 5 wt% HA and Mg-1 wt% Sn-5 wt% HA composites were prepared separately by stir assisted squeeze casting route. The phase analysis and microstructure were characterized by X-ray diffraction (XRD) and scanning electron microscope (SEM) coupled with energy dispersive spectroscopy (EDS) respectively. Mechanical properties were evaluated by conducting the compression and micro hardness tests. Corrosion properties of as-cast composites were studied by linear polarization, Tafel and electrochemical impedance spectroscopy (EIS) techniques. The results of both XRD and SEM-EDS revealed that the main constitutional phases of as-cast Mg/HA composites were α-Mg and HA whereas, in Mg-Sn/HA composites, the phase Mg_2Sn was observed along with fine distribution of HA particles. In both the cases, no interfacial reactions observed. The yield strength, ultimate compression strength and hardness were found to be increased with the addition of Sn in Mg/HA composites. Furthermore, the addition of Sn also played an important role in increasing the corrosion resistance of the Mg/HA composites which was attributed the refinement of grain size and the formation of Mg_2Sn phase along the grain boundaries. Hence, it was concluded that the addition of Sn improves both mechanical and corrosion properties of Mg/HA composites.

Keywords: Magnesium; Composite; Biomedical; Corrosion; Squeeze casting.

1. Introduction

Mg and their alloys are gaining much interest in the field of biomaterials recently due to their favourable properties such as biocompatibility, degradability, nontoxicity besides their high strength to weight ratio, closer value of elastic modulus to that of natural bone etc. However, their low bioactivity and high corrosion rates limit their applications as biomaterials [1]. On the other hand, hydroxyapatite (HA) is well known for its bioactivity which helps in the osseointegration of the bone. Many researchers have studied various processes to coat the surface of Mg alloys with hydroxyapatite in order to improve their bioactivity [2]. However, the studies on Mg based biocomposites, especially, studies on Mg/HA composites are very limited in the literature. The major problem with reinforcing HA in Mg matrix could be the loss of ductility which in turn effects the yield strength. Furthermore, it is also well known that the corrosion rates of the Mg alloy will be higher when reinforced with secondary phases in the form of particles or fibres. Most of the previous reports suggested that the increase in HA shows a negative effect on the compression strength due to the agglomeration of HA particles and it also acts as galvanic couple induces the intensity of degradation rate results in the detachment of apatite layer [3–5].

* Corresponding author.
E-mail address: sreekanth.dondapati@vit.ac.in (D. Sreekanth).

https://doi.org/10.1016/j.jma.2019.05.010

Prakash et al. [6] prepared the porous Mg-Zn-Mn-HA composites by spark plasma sintering process and reported that the developed composites exhibits the mechanical properties such as elastic modulus (29–59HV) and hardness (30-HV) closer to the bone properties and shows good bioactivity and corrosion resistance. It was also found that the corrosion resistance of such composites be improved by addition of Si and HA and the reasons were attributed to the formation of CaMg, $MgSi_2$ phases which restricts the degradation of material in SBF and also shows the improvement in growth and proliferation of osteoblastic cells [7]. Wang et al., investigated the porous Mg-5Sn-(HA+βTCP) composites processed through infiltration technique and observed that the pits were entirely covered by the corrosion products of HA and magnesium hydroxide ($Mg(OH)_2$) leads to increase the corrosion resistance than Mg-5Sn alloy [8,9]. Lim et al. [10] developed Mg-1Ca-(5,10,15 wt%)HA composites through powder processing route and they reported that Mg-1Ca-10HA shows excellent cell viability and bioactivity. However, higher amount of HA addition (more than 10 wt%) leads to the deterioration of corrosion resistance due to the increase in anodic sites [11]. However, alloying of magnesium with the elements such as Sn, Zn, Ca etc. seems to have positive effect on improving the corrosion resistance. However, much research has been recently focused on Tin (Sn) as an alloying element for Mg and reported that it improves corrosion resistance, mechanical properties, castability by the formation of the Mg_2Sn [12–14]. Furthermore, Sn is a trace element in human nutrition and can interfere with the metabolism of Zn, Ca and Cu which makes it more favourable for the applications as biomaterial. Zhao et al. [15] reported that Mg-1Sn alloy shows homogenous grain structure, favourable strength, elongation, level of toxicity for orthopaedic applications compared to Mg-Sn (5,7 wt%) alloys produced by sub rapid solidification process. Further, it was also found that compression strength, hardness and degradation rate in Simulated body fluid (SBF) was favourable when Sn content in Mg is less that 5 wt% [16–19]. Zhao et al. [20] concluded that addition of 1 wt% Sn and 0.5 wt% Ca in pure Mg results in uniform grain structure, better mechanical and corrosion properties due to the lesser amount of intermetallic phases. Furthermore, fabrication of magnesium alloy and its composite is the great challenge for engineers and scientist because of the high affinity of magnesium towards oxygen. Few scientists have studied the possibility of making these composites by powder metallurgy route [8] and very few studies are available on the other routes such as casting and infiltration techniques [10,21]. On the hand, squeeze casting (SC) is regarded as a net-shape fabrication route mainly related to aluminium and magnesium-based alloys with special emphasis on metal matrix composites (MMCs) in which solidification occurs rapidly by the application of pressure which in turn produce fine grained structure with minimal porosity [22,23,24].

Hence, in the present study, Mg/HA composites were prepared by stir assisted squeeze casting route. In order to see the feasibility of improving the mechanical and corrosion behaviour of composites, 1 wt% of Sn was added and analysed.

2. Materials and methods

2.1. Fabrication of composites

The preparation of nano sized hydroxyapatite by microwave synthesis method is described elsewhere [25]. Analytical grade calcium hydroxide [$Ca(OH)_2$, E. Merck, Germany] and di-ammonium hydrogen phosphate [DAP, $(NH_4).2HPO_4$, E. Merck, Germany] were used for the preparation of HA nanoparticles by microwave processing. The amount of the reactants was calculated based on the Ca/P molar ratio of 10/6. After the synthesis of HA powders, they were stored carefully in the desiccator till the time of use to avoid any carbonation. For the fabrication of composites, the pure Mg and 1 wt% Sn ingots of 99% purity are charged in the preheated crucible which is operated by microprocessor based electrical resistance furnace under controlled inert argon gas atmospheric conditions. The 5 wt% of HA powder is preheated to 300 °C for 60 min and added in Mg-Sn melt measuring 820 °C. The twin blade stirrer made of stainless steel was operated at 400 rpm for 20 min with 5 min step to ensure the homogeneous dispersion of reinforcements in the Mg-Sn alloy matrix. The molten Mg-Sn/HA composite has been transferred to the mild steel mould preheated to 300 °C through the inclined hopper at the bottom of the furnace. A 40 Tons hydraulic press was then operated to plunge the piston for squeezing the molten metal at the pressure of 150 MPa for 60 s. The rapid solidification of the melt occurs through the application of pressure and the cast composite sample was ejected. Mg with 5 wt% HA composite without adding Sn was also fabricated in a similar manner.

2.2. Phase identification and microstructure

Identification of phases present in Mg/HA and Mg-Sn/HA cast composites was carried out by XRD pattern analysis which were obtained by X-ray diffractometer (X'pert Pro, PANalytical, The Netherlands) with Cu Kα radiation (λ = 0.1540598 nm) at 45 kV and 30 mA. The scan speed of 1° /min and a step size of 0.05° over the 2θ range of 20°–90° were employed during the scanning. SEM attached with EDS (EVO/18, Zeiss) was used to observe the surface morphologies of all the samples.

2.3. Mechanical characterization

The cylindrical specimens with L/D ratio ~1 are subjected to compression test as per ASTM E9-89A in Schimadzu servo controlled machine with a cross head speed of 0.04 mm/min and the ultimate compression strength, yield strength, fracture strain, and modulus for all the samples were obtained. Vickers microhardness measurement was carried out on the samples by using Shimadzu automatic digital microhardness tester as per ASTM E8 using 25 gf indenting load with dwell time of 15 s. Each test was repeated five times and the average values of results have been presented in Table 1.

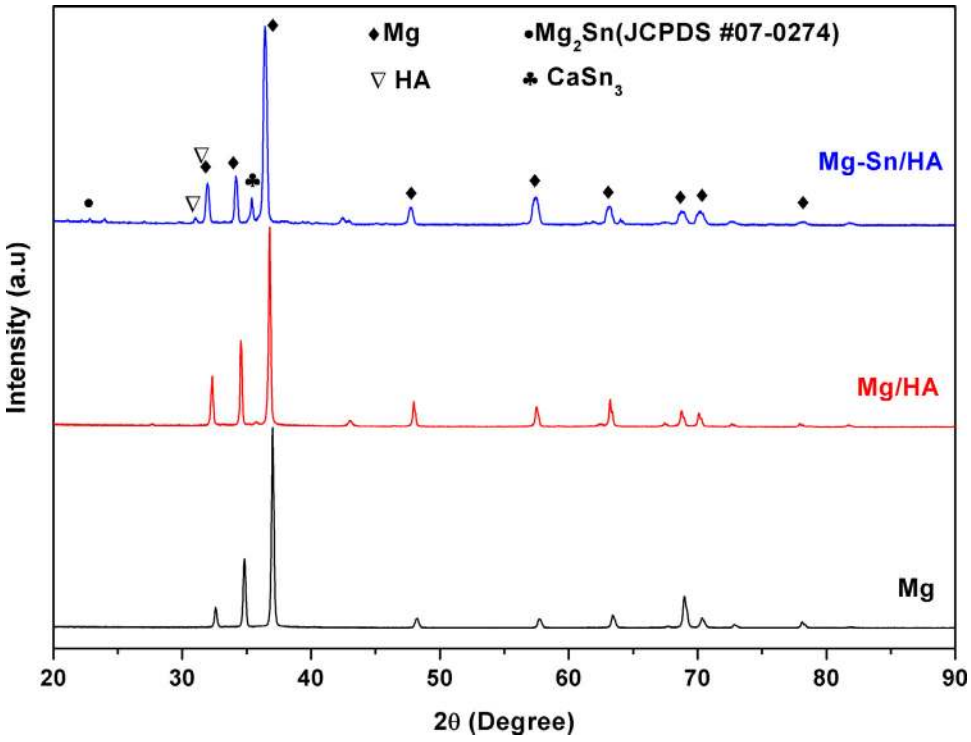

Fig. 1. XRD patterns of pure Mg, Mg-HA and Mg-Sn/HA composites.

Table 1
Mechanical properties of pure Mg, Mg/HA and Mg-Sn/HA composites.

Sample	UCS (N/mm^2)	YS (N/mm^2)	Fracture strain (%)	Elastic modulus (GPA)	Microhardness (Hv)
Mg	154.60	108	38.96	10	62.3
Mg/HA	250.185	98	11.11	37.5	86.21
Mg-Sn/HA	278.55	196	8.03	66.6	96.25

2.4. Corrosion and electrochemical tests

The linear polarization, Tafel analysis and EIS tests were conducted in SBF medium at 35 °C using a potentiostat (Interface 1010, Gamry Instruments) by exposing 0.5 cm^2 area of the sample. The composition and preparation of the Kokubo's SBF were as given in the reference [26]. The corrosion cell consisted of a saturated calomel electrode (SCE) and a platinum wire, as reference and counter electrodes respectively. For linear polarization resistance experiment was conducted by scanning in the range of ± 20 mV about E_{corr} (the open circuit potential) at a scan rate of 0.1 mV/sec. The plots were then drawn between applied potential vs. the measured current. Tafel plots were generated by polarizing the specimen about 0.2 V anodically and cathodically with reference to open circuit potential (OCP) at a scan rate of 0.5 mV s^{-1} after an initial delay of 60 min. EIS measurements were made from a start frequency of 10^4 Hz up to 0.1 Hz with AC signal amplitude of 10 mV rms. After the measurements were obtained, the Tafel and impedance data were analysed by curve fitting and equivalent circuit modelling using Gamry Echem Analyst software.

3. Results and discussion

3.1. Morphology and phase analysis

Fig. 1 shows the XRD pattern of as-cast pure Mg, Mg/HA and Mg-Sn/HA composites. The characteristic peaks of HA at $2\theta = 31.7°$, 32.19° as per the standard pattern of HA (JCPDS#: 09–432) were clearly observed in the XRD patterns of Mg/HA and Mg-Sn/HA. Apart from HA peaks, a low intensity peak at $2\theta = 22.74°$ was found which matched with the standard pattern of Mg_2Sn (JCPDS#: 07–0274) confirming the presence of Mg_2Sn phase in Mg-Sn/HA composite. However, the very low intensity peaks corresponding to HA and Mg_2Sn implies their presence in lower volume fraction. Furthermore, $CaSn_3$ phase was also identified at $2\theta = 35.56°$ which indicates partial dissociation of HA and the reaction of Ca from HA with Sn.

Fig. 2(a) and (b) shows the SEM micrographs of Mg/HA and Mg-Sn/HA samples respectively. In both the images uniformly dispersed spherical particles of HA in Mg matrix are observed whereas, in the image of Mg-Sn/HA, the phase Mg_2Sn can also be observed in α-Mg matrix along the grain boundaries. Higher the electronegative difference between the elements, greater the possibility of formation of intermetallic phases. Owing to this phenomenon of electronegative difference between Mg and Sn is 0.65, the formation of Mg_2Sn is easier and it was revealed by the XRD pattern of Mg-Sn/HA composite. The minor amount of agglomeration of

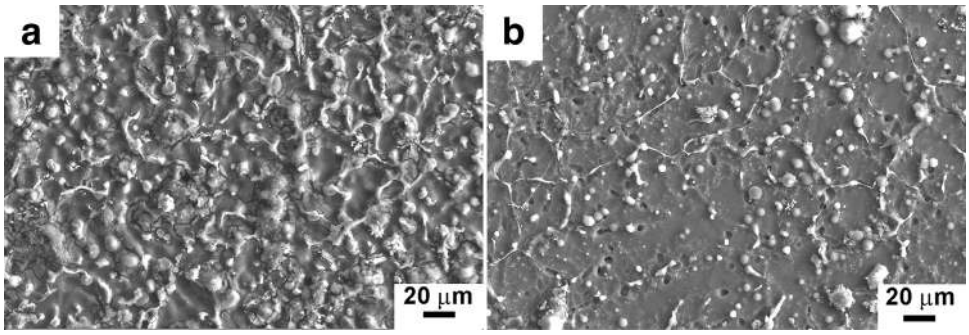

Fig. 2. SEM micrographs of (a) Mg/HA and (b) Mg-Sn/HA samples.

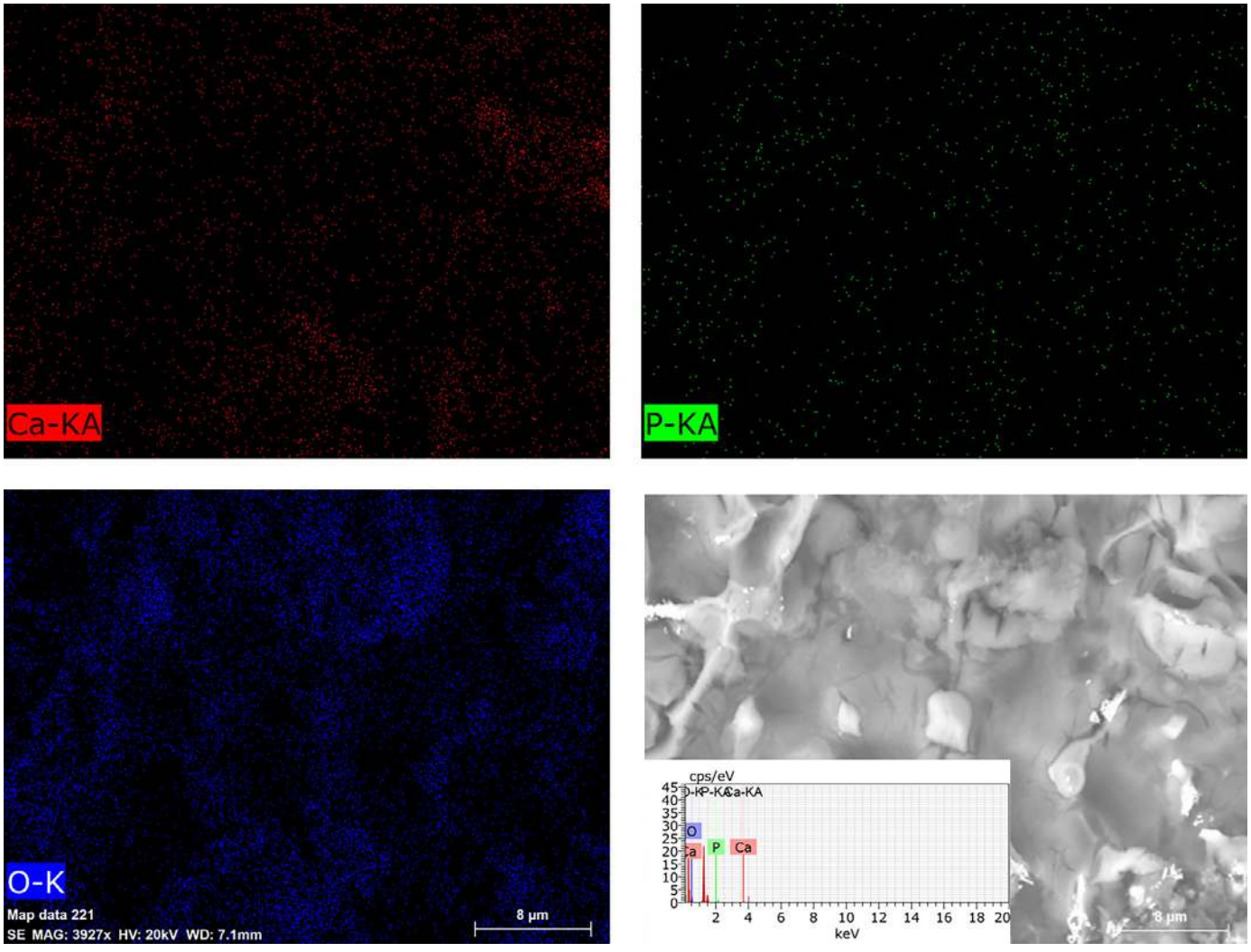

Fig. 3. EDS elemental mapping of Mg/HA surface.

HA particles can also be observed randomly in both the composites. However, when compared to the microstructure of Mg/HA, the microstructure of Mg-Sn/HA seems to be more refined with well distribution of HA particles in α-Mg matrix. The same was confirmed by the results of EDS as shown in Fig. 3 and 4 where the distribution of the phases is evident. Further, the EDS results also confirms the presence and well distribution of HA particles and Mg_2Sn phase by identifying Ca, P, O and Sn respectively.

3.2. Mechanical properties

Table 1. lists the various mechanical properties of the composites under this study such as, ultimate compression

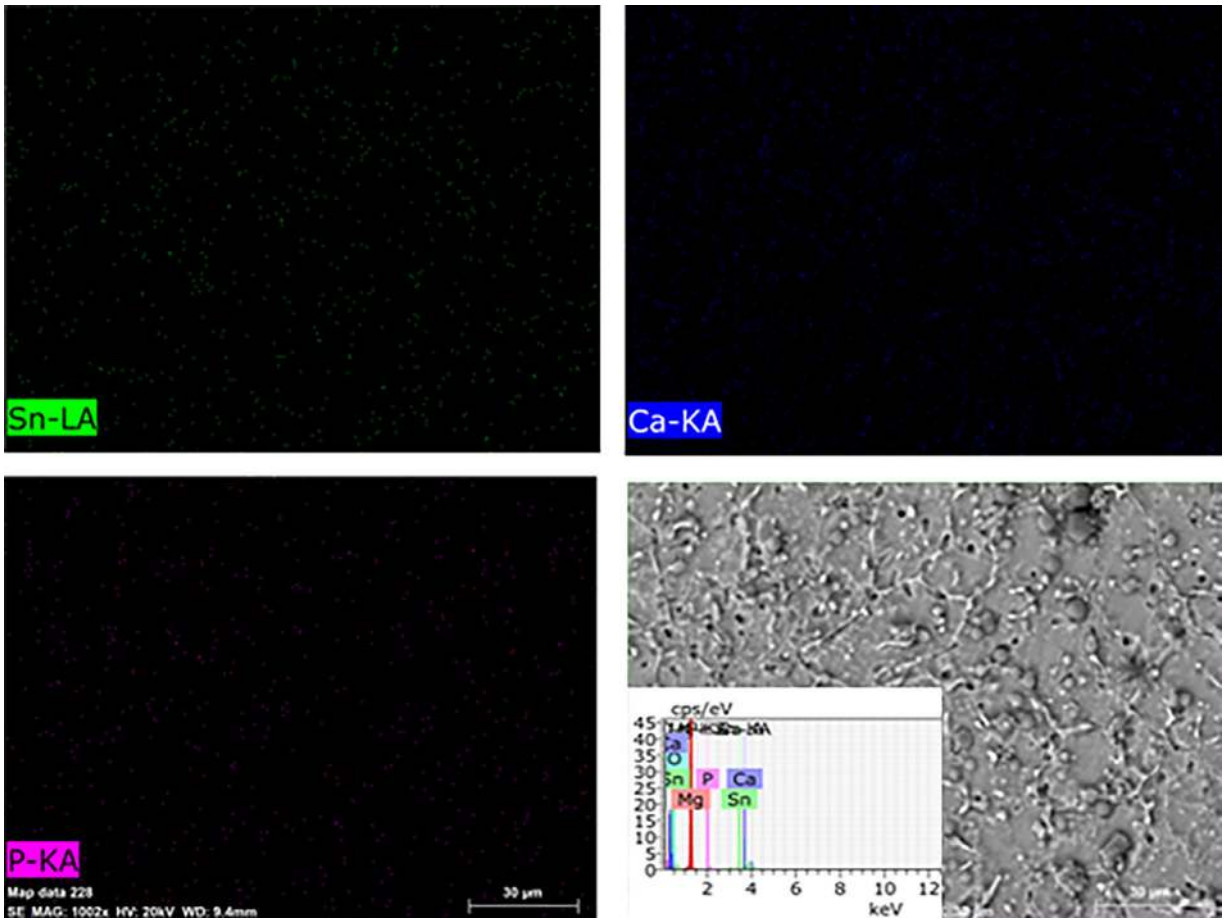

Fig. 4. EDS elemental mapping of Mg-Sn/HA surface.

strength (UCS), yield strength (YS), fracture strain (FS), elastic modulus, and hardness. It can be seen that the hardness of the composites has increased significantly as compared to that of pure Mg. The addition of HA leads to restrict the movement of dislocations which might be the reason for improving the hardness of pure monolithic Mg. Also, it's worth noting that minor addition of Sn increases the hardness value of Mg/HA composites are attributed to grain refinement due to the addition Sn and the occurrence of hard intermetallic Mg_2Sn precipitates which distributed uniformly in the matrix. Magnesium matrix composites exhibit higher strength which indicates that the load is being transferred to the strong reinforcement particles reducing the stress carried by the matrix. The hard HA particles barricades the dislocations within the grains and also resists the deforming stress thus enhancing compressive strength of the composite. Moreover, highly dispersed HA particles in α-Mg matrix restricts the plastic flow and surrounds the eutectic phases could have contributed to the increase in compression strength. The ultimate compression strength of Mg-Sn/HA composites was higher than Mg/HA which may be attributed to the solid interfacial bonding between Mg and HA offered by the addition of Sn which has good wettability with Mg. The yield strength was measured at 0.2% strain offset for all the samples and was observed that yield strength of Mg-Sn/HA was higher than Mg/HA composites owing to the presence of Mg_2Sn and HA particles which facilitates the pinning action that hinders the twinning phenomenon. It can also be noted from Table 1 that the modulus of elasticity of Mg was increased with the addition of HA and further increased with the addition of 1 wt% Sn, the value of which is close to that of natural bone, helps in reducing stress shielding effect. Furthermore, compared to Mg, the fracture strain was lesser in Mg/HA and Mg-Sn/HA composites which is generally the case with the MMCs. However, the decrease in fracture strain is not an important parameter to be considered for biomedical applications.

3.3. Corrosion studies

Linear polarization curves were obtained by scanning through a potential range, that is $\pm$ 25 mV about E_{corr} and the resulting current is plotted versus potential, as shown in Fig. 5. The corrosion current, I_{corr}, is related to the slope of

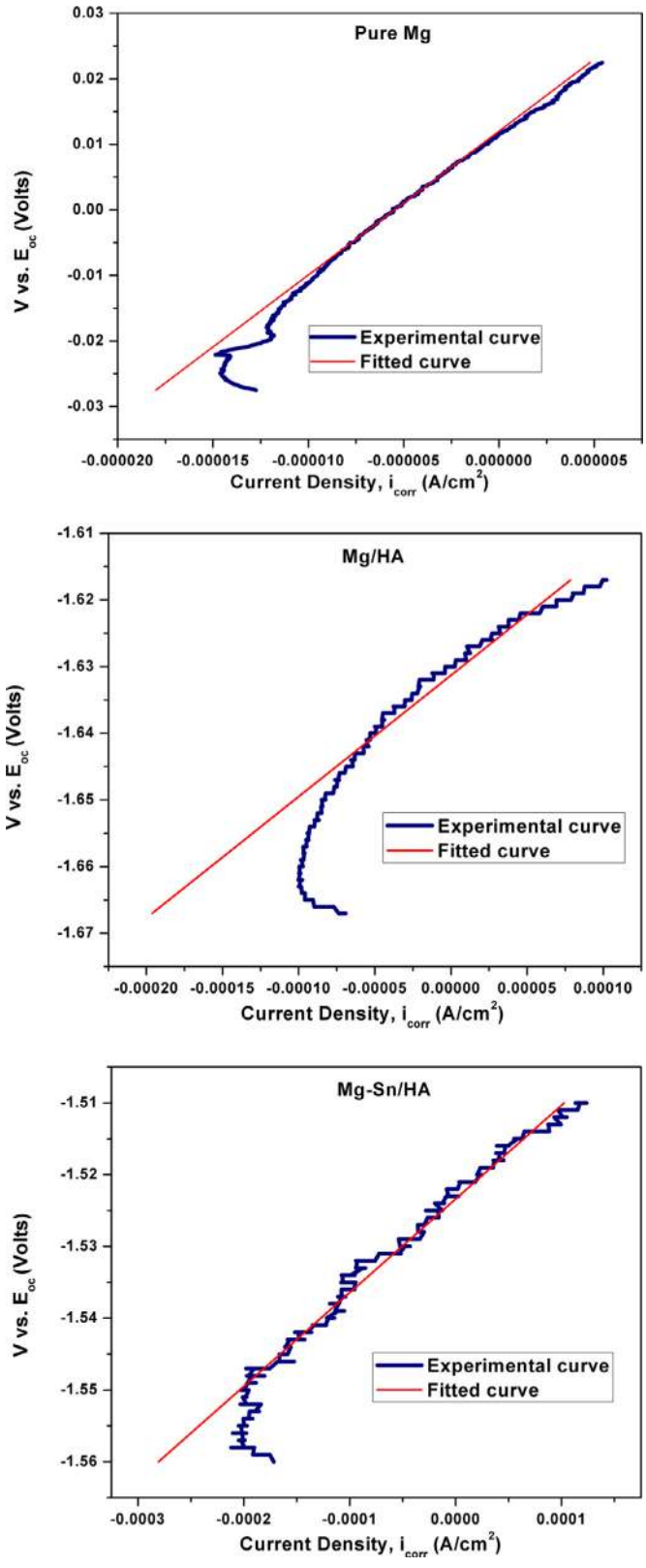

Fig. 5. Linear polarization curves of pure Mg, Mg/HA and Mg-Sn/HA samples.

the plot through the following equation:

$$\frac{\Delta E}{\Delta I} = \frac{\beta a \times \beta c}{2.3(Icorr)(\beta a + \beta c)} \quad (1)$$

Polarization resistance was obtained by taking the slope of the curves. Tafel plots shown in Fig. 6 were also drawn to determine the anodic and cathodic Tafel constants β_a and β_c respectively. Using these values corrosion rate was determined using the equation:

$$\text{Corrosion Rate(mpy)} = 0.13\, I_{corr}(\text{E.W.})/d \quad (2)$$

Where,

E.W.=equivalent weight of the corroding species, g.
d=density of the corroding species, g/cm^2.
I_{corr}=corrosion current density, μA/cm^2

The corrosion data obtained from both linear polarization and Tafel tests are presented in Tables 2 and 3 respectively. The appearance of the polarisation curves clearly indicate that there is no passivation of the surface in case of pure Mg sample but there is a slight passivating nature observed in case of both Mg/HA and Mg-Sn/HA samples. Further, the pH value after a period of 60 min. was observed to be 8.00 and 7.64 for Mg/HA and Mg-Sn/HA composites respectively indicate that the sample containing Sn has tendency to reduce the hydrogen evolution. It can also be noted that there is no pitting occurred for any of the samples under the study. It is evident that the addition of HA to Mg matrix has largely reduced the corrosion resistance of magnesium as it is known that most of the common reinforcements reduce the corrosion resistance of Mg alloys. However, it seems that the addition of Sn to the composite has reduced the corrosion rate to 354.9 mpy from 1311 mpy observed for Mg/HA sample.

The Nyquist and Bode plots of experimental and fitted curves of samples under the study are shown in Fig. 7. The equivalent circuit which best fits the experimental data is shown in Fig. 8 and corresponding EIS data is presented in Table 4. This circuit is suitable for all tested electrodes. In the equivalent circuit (Fig. 8), R_u, R_p correspond to solution resistance offered by corrosive electrolyte and polarization resistance of the sample respectively. The presence of displaced semicircles suggests a non-ideal behaviour of the capacitor, leading to the introduction of a constant phase element (CPE) in the equivalent circuits. Constant-phase element (CPE) is used in parallel to R_p instead of pure capacitor. CPE is extensively used in equivalent electrical circuits for fitting of experimental impedance data owing to distributed surface reactivity, surface inhomogeneity, roughness or fractal geometry, electrode porosity, and to current and potential distributions associated with electrode geometry which results in frequency dispersion. In the present case, the use of CPE can be attributed to inhomogeneous distribution of grains. CPE is given by $Z_{CPE} = [Y_0(j\omega)\alpha]^{-1}$, where $-1 \leq \alpha \leq 1$. The value of α is associated with the non-uniform distribution of current as a result of both the degree of roughness of the surface and is also well known that the CPE is considered as pure capacitor if $\alpha = 1$ and pure resistor if $\alpha = 0$. As can be observed from Table 4, values of α for all the samples suggests

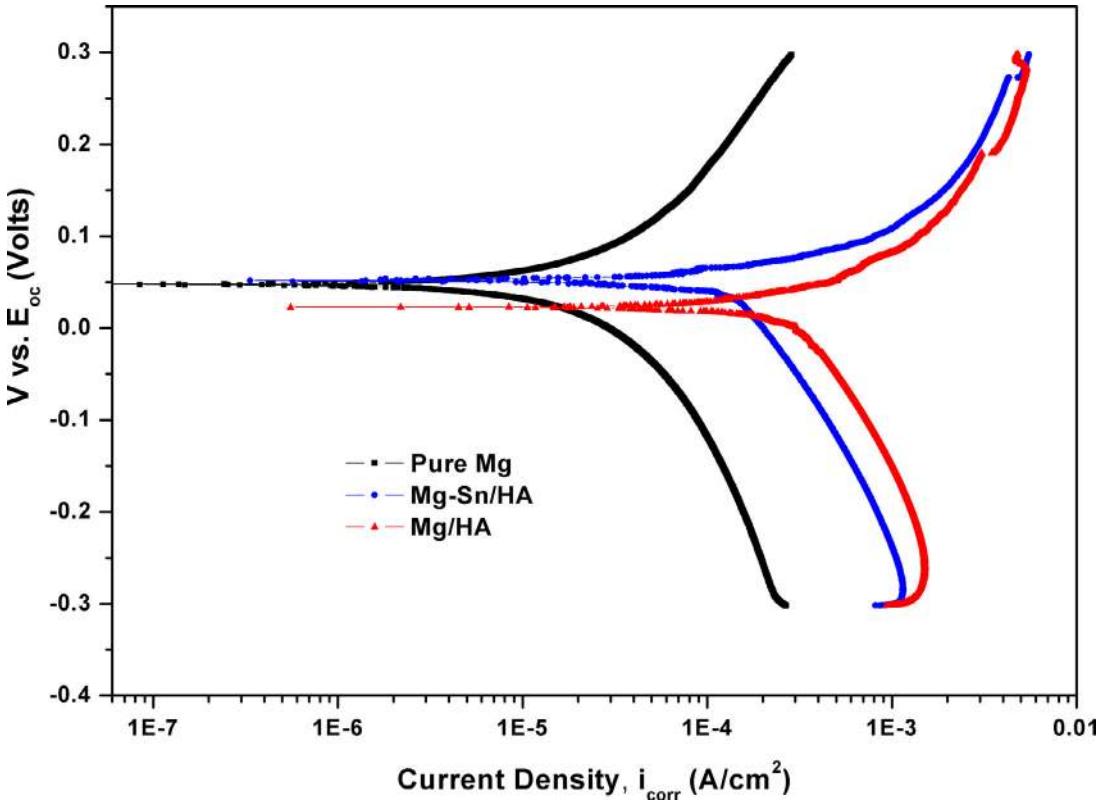

Fig. 6. Potentiodynamic polarization curves of pure Mg, Mg/HA and Mg-Sn/HA samples.

Table 2
Electrochemical parameters obtained from linear polarization curves.

Sample	β_a (V/decade)	β_c (V/decade)	R_p (Ω-cm^2)	I_{corr} (μA/cm^2)	E_{corr} (V)	Corrosion rate (mpy)
Mg	0.3774	0.5812	4343	22.88	−1.8	40.93
Mg/HA	0.2535	1.677	130.5	732.7	−1.5	1311
Mg-Sn/HA	0.1152	0.7779	219.6	198.4	−1.6	354.9

Table 3
Electrochemical parameters obtained from potentiodynamic polarization curves.

Sample	β_a (V/decade)	β_c (V/decade)	I_{corr} (μA/cm^2)	E_{corr} (V)
Mg	0.3774	0.5812	32.10	−1.8
Mg/HA	0.2535	1.677	900	−1.5
Mg-Sn/HA	0.1152	0.7779	402.00	−1.6

Table 4
Equivalent circuit fitting results of EIS data for pure Mg, Mg/HA and Mg-Sn/HA samples.

Sample	R_p (Ohms)	R_u (Ohms)	Y_0 (S*s^a)	α
Mg	4232	120.4	351×10^{-7}	0.728
Mg/HA	900	110	236×10^{-7}	0.7853
Mg-Sn/HA	1320	103.6	122×10^{-7}	0.8451

the capacitance behaviour. Solution resistance of all the samples are nearly same and suggests that the experiments were conducted under similar condition of electrolyte. The trend of polarization resistance (R_p) as seen from Table 4 conforms to the results obtained from both linear polarization and Tafel plots. The decrease of CPE (Y_0) for Mg-Sn/HA sample as compared to both pure Mg and Mg/HA samples suggests that the penetration of the aggressive ions in the solution into the alloy was mitigated by passive film, consequently resulting in higher pitting resistance. Similar trend was observed even from the Tafel plots as discussed in the above sections.

From the results of corrosion test linear polarization, Tafel and EIS, it can be clearly understood that the reinforcement of HA in Mg matrix would reduce the corrosion resistance and addition of Sn as an alloying element helps in increasing the corrosion resistance of the composite. This could be attributed to the grain refinement and the formation of Mg_2Sn phase due to the addition of Sn as revealed by both XRD and SEM-EDS results.

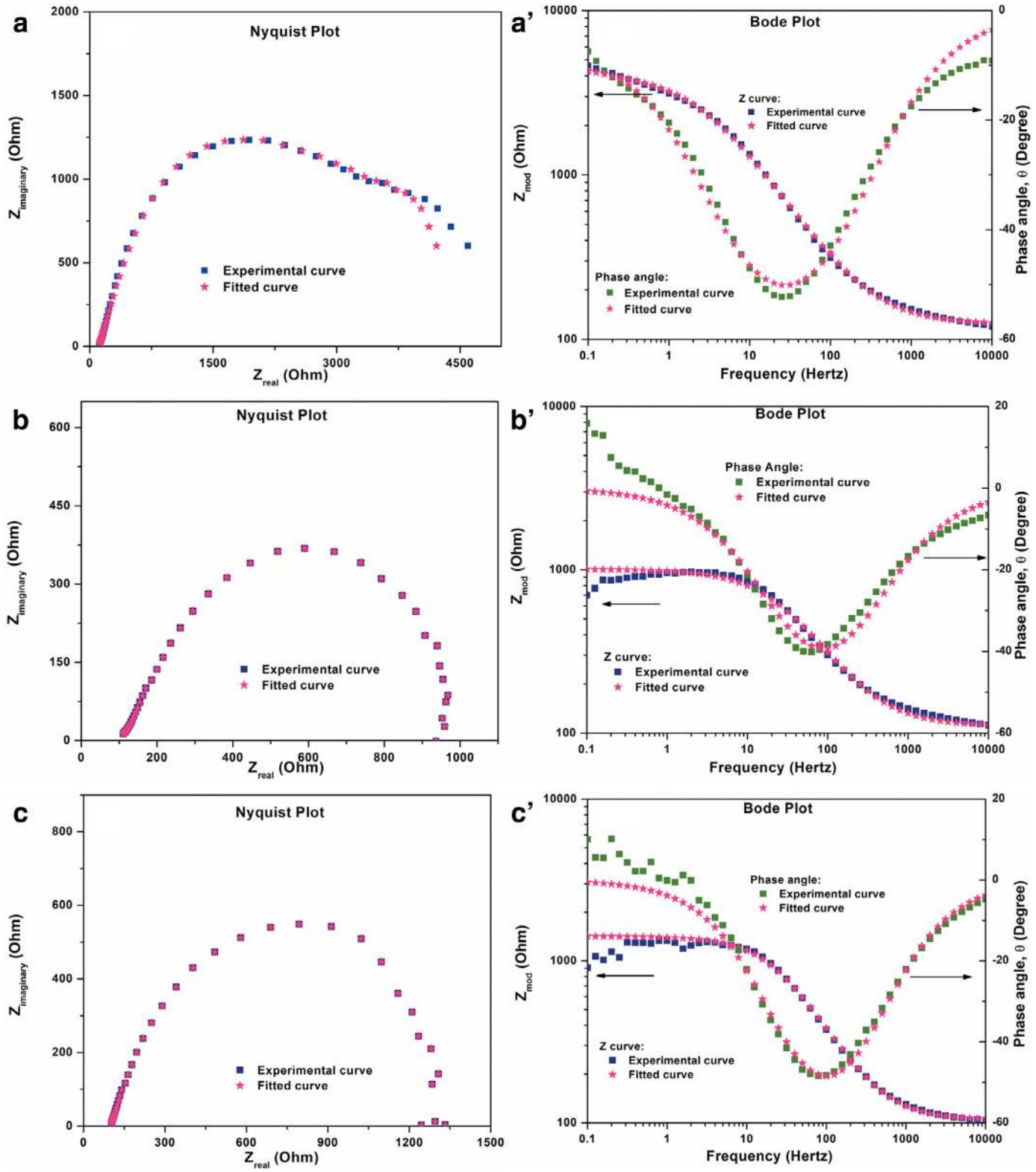

Fig. 7. Nyquist and Bode curves of pure Mg, Mg/HA and Mg-Sn/HA samples from EIS tests.

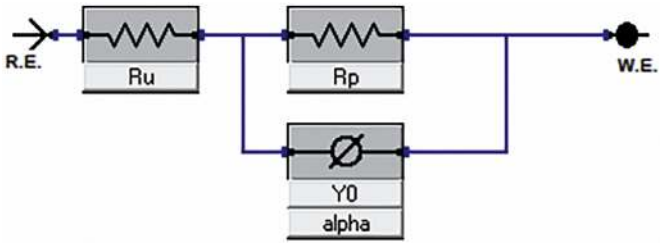

Fig. 8. Equivalent circuit used for fitting the EIS curves of pure Mg, Mg/HA and Mg-Sn/HA samples.

4. Conclusions

The current study indicates that the Mg/HA and Mg-Sn/HA composites were successfully produced by stir assisted squeeze casting route with minimum defects. The process was found to be efficient in producing the composites with the uniform distribution of HA particles with good interfacial bonding between the matrix and reinforcement. The significant changes in microstructure and refinement of grain size has been observed due to the addition of Sn to Mg/HA composites. Mechanical properties such as compression strength, yield strength and hardness have been improved by reinforcing HA into Mg matrix and further improved by the addition of Sn to Mg/HA composites. Linear polarization, potentiodynamic polarization and EIS results suggested that the reinforcing HA into Mg matrix deteriorated the corrosion resistance of Mg and the addition of 1 wt% Sn was helpful in decreasing the corrosion rates. However, the effect of addition of more weight percentage of Sn on corrosion behaviour and biocompatibility are yet to be studied.

Funding

This research did not receive any specific grant from funding agencies in the public, commercial or not-for-profit sectors.

Declaration of Competing Interest

There is no conflict of interest.

Acknowledgements

The authors would like to thank the management of Vellore Institute of Technology, Chennai for the support provided for this research.

References

[1] R. Radha, D. Sreekanth, J. Magnes. Alloys 5 (2017) 286–312.
[2] D. Sreekanth, N. Rameshbabu, K. Venkateswarlu, Ceram. Int. 38 (2012) 4607–4615.
[3] D. Sreekanth, N. Rameshbabu, Mater. Lett. 68 (2012) 439–442.
[4] S. Jaiswal, R. Manoj Kumar, P. Gupta, M. Kumaraswamy, P. Roy, D. Lahiri, J. Mech. Behav. Biomed. Mater. 78 (2018) 442–454.
[5] A.S. Sabet, A.H. Jabbari, M. Sedighi, J. Compos. Mater. 52 (2018) 1711–1722.
[6] N. Aboudzadeh, Ch Dehghanian, M. Shokrgozar, Iran. J. Mater. Sci. Eng. (2017) 14.
[7] P. Chander, S. Singh, K. Verma, S.S. Sidhu, S. Singh, Vacuum 155 (2018) 578–584.
[8] P. Chander, S. Singh, I. Farina, F. Fraternali, L. Feo, PSU Res. Rev. 2 (2018) 152–174.
[9] X. Wang, J.T. Li, M.Y. Xie, L.J. Qu, P. Zhang, X.L. Li, Mater. Sci. Eng., C. 56 (2015) 386–392.
[10] J.-X. Li, Y. Zhang, J.-Y. Li, J.-X. Xie, J. Mater. Sci. Technol. 34 (2018) 299–310.
[11] P.N. Lim, R.N. Lam, Y.F. Zheng, E.S. Thian, Mater. Lett. 172 (2016) 193–197.
[12] X. Gu, W. Zhou, Y. Zheng, L. Dong, Y. Xi, D. Chai, Mater. Sci. Eng., C. 30 (2010) 827–832.
[13] Z. Zhen, T. Xi, Y. Zheng, L. Li, L. Li, J. Mater. Sci. Technol. 30 (2014) 675–685.
[14] H.-Y. Ha, J.-Y. Kang, S.G. Kim, B. Kim, S.S. Park, C.D. Yim, B.S. You, Corros. Sci. 82 (2014) 369–379.
[15] J. Kubásek, D. Vojtěch, J. Lipov, T. Ruml, Mater. Sci. Eng., C. 33 (2013) 2421–2432.
[16] C. Zhao, F. Pan, S. Zhao, H. Pan, K. Song, A. Tang, Mater. Des. 70 (2015) 60–67.
[17] Y. Zhou, P. Wu, Y. Yang, D. Gao, P. Feng, C. Gao, H. Wu, Y. Liu, H. Bian, C. Shuai, J. Alloys Compd 687 (2016) 109–114.
[18] C. Zhao, F. Pan, S. Zhao, H. Pan, K. Song, A. Tang, Mater. Des. 70 (2015) 60–67.
[19] C. Zhao, F. Pan, S. Zhao, H. Pan, K. Song, A. Tang, Mater. Sci. Eng., C. 54 (2015) 245–251.
[20] H.-Y. Ha, J.-Y. Kang, J. Yang, C.D. Yim, B.S. You, Corros. Sci. 102 (2016) 355–362.
[21] C.-Y. Zhao, F.-S. Pan, H.-C. Pan, Trans. Nonferrous Met. Soc. China. 26 (2016) 1574–1582.
[22] Q. Yuan, Y. Huang, D. Liu, M. Chen, Bioelectrochemistry 124 (2018) 93–104.
[23] A.K.S. Bankoti, A.K. Mondal, S. Kumar, B.C. Ray, Mater. Sci. Eng., A. 626 (2015) 186–194.
[24] D. Yuan, X. Yang, S. Wu, S. Lü, H. Kun, J. Mater. Process. Technol. 269 (2019) 1–9.
[25] N. Rameshbabu, K. Prasad Rao, T.S. Sampath Kumar, J. Mat. Sci. 40 (2005) 6319–6323.
[26] T. Kokubo, H. Takadama, Biomaterials 27 (2006) 2907–2915.